Gas-Phase Conformations of Deprotonated Trinucleotides ($dGTT^-$, $dTGT^-$, and $dTTG^-$): The Question of Zwitterion Formation

Jennifer Gidden and Michael T. Bowers
Department of Chemistry and Biochemistry, University of California, Santa Barbara, California, USA

The gas-phase conformations of a series of trinucleotides containing thymine (T) and guanine (G) bases were investigated for the possibility of zwitterion formation. Deprotonated $dGTT^-$, $dTGT^-$, and $dTTG^-$ ions were formed by MALDI and their collision cross-sections in helium measured by ion mobility based methods. $dTGT^-$ was theoretically modeled assuming a zwitterionic and non-zwitterionic structure while $dGTT^-$ and $dTTG^-$ were considered "control groups" and modeled only as non-zwitterions. In the zwitterion, G is protonated at the N7 site and the two neighboring phosphates are deprotonated. In the non-zwitterion, G is not protonated and only one phosphate group is deprotonated. Two conformers, whose cross-sections differ by 17 ± 2 Å^2, are observed for $dTGT^-$ in the 80 K experiments. Multiple conformers are also observed for $dGTT^-$ and $dTTG^-$ at 80 K, though relative cross-section differences between the conformers could not be accurately obtained. At higher temperatures (>200 K), the conformers rapidly interconvert on the experimental time scale and a single "time-averaged" conformer is observed in the ion mobility data. Theory predicts only one low-energy conformation for the zwitterionic form of $dTGT^-$ with a cross-section 8% smaller than experimental values. Additionally, the extra H^+ on G does not bridge both phosphates. Thus, $dTGT^-$ does not appear to be a stable zwitterion in the gas-phase. Theory does, however, predict two low-energy conformers for the non-zwitterionic form of $dTGT^-$ that differ in cross-section by 18 ± 3 Å^2, in good agreement with the experiment. In the smaller cross-section form (folded conformer), G and one of the T bases are stacked while the other T folds towards the stacked pair and hydrogen bonds to G. In the larger cross-section form (open conformer), the unstacked T extends away from the T/G stacked pair. Similar folded and open conformers are predicted for all three trinucleotides, regardless of which phosphate is deprotonated. (J Am Soc Mass Spectrom 2003, 14, 161–170) © 2003 American Society for Mass Spectrometry

Mass spectrometry has proven to be extremely useful for characterizing biological molecules in the gas phase. Although most of these applications involve the sequence and structural analysis of peptides and proteins, interest is growing in using mass spectrometry to analyze DNA [1–3]. However, MS studies on DNA have been hindered because of the tendency of the polynucleotides to fragment during the MALDI [4] process of ion formation, lowering signal intensities and peak resolution. This fragmentation problem generally limits the size of the polynucleotide that can be routinely studied by mass spectrometry to ~100 bases in length and creates difficulties in monitoring small structural changes such as the methylation of a base or detecting mutations along the DNA chain.

Several groups have investigated this fragmentation problem with the hope of developing strategies to fix it. New matrices have shown some success in decreasing the amount of fragmentation [5–7] as have adding ammonium salts to the DNA sample [8–11] and the use of IR-MALDI ioniziation sources [12, 13], which have yielded mass spectra of polynucleotides containing more than 1000 bases. Other studies, however, have focused on smaller oligonucleotides to determine the exact mechanism of the fragmentation. It is believed that the fragmentation is initiated by the protonation, and subsequent elimination, of one of the bases in the oligonucleotide chain, followed by multiple cleavages of the sugar-phosphate backbone [14–16].

Hillenkamp, Gross, and co-workers investigated the fragmentation of several protonated and deprotonated oligonucleotides using post source decay and H/D exchange [17, 19]. They concentrated on a series of tetranucleotides containing one guanine (G) base and three thymine (T) bases [17, 19]. The reason for this is that G has the highest proton affinity of the DNA bases

Published online January 14, 2003
Address reprint requests to Dr. M. T. Bowers, Department of Chemistry and Biochemistry, University of California, Santa Barbara, CA 93106-9530, USA. E-mail: bowers@chem.ucsb.edu

1044-0305/03/$30.00
doi:10.1016/S1044-0305(02)00866-8

Received September 5, 2002
Revised November 21, 2002
Accepted November 21, 2002

while T has the lowest [20] and so G should be the base that is eliminated in the proposed fragmentation scheme. For the protonated tetranucleotides [17], the mass spectra showed that a protonated (deuterated) G was indeed eliminated, regardless of where G was positioned in the tetranucleotide chain (dGTTT, dTGTT, dTTGT, or dTTTG). However, for the deprotonated ions [18], the mass spectra for $dGTTT^-$ and $dTTTG^-$ showed loss of G while the spectra for $dTGTT^-$ and $dTTGT^-$ showed loss of T instead. It was proposed that $dTGTT^-$ and $dTTGT^-$ formed zwitterions, with G protonated and the two neighboring phosphate groups deprotonated, which stabilized the glycosidic bond and prevented the loss of G from occurring.

When investigating the fragmentation of large biomolecules it is important to consider not only the primary structure and sequence of the molecule but its overall shape as well. Atoms that appear to be close together in a 2-D rendition of the molecule may not be close when the molecule folds into its desired 3-D conformation. Higher-order structural features of peptides have been known to affect collision-induced dissociation spectra and influence sequence assignments and fragmentation mechanisms [21–24]. While many studies have investigated the gas-phase conformations of peptides [25–32] and proteins [33–35], very few have focused on oligonucleotides [36].

Our original goal was to use mass spectrometry and ion mobility methods [37, 38] to examine the gas-phase conformations of the above-mentioned T/G tetranucleotides to determine whether $dTGTT^-$ and $dTTGT^-$ form zwitterions as predicted. However, since so little data is available on the conformations of oligonucleotides in the gas phase, we began with the more straightforward dinucleotides [39, 40]. The results indicated that even these relatively simple systems have complex conformational and energetic properties (up to three conformations were identified for some of the dinucleotides). Therefore, the next step we elected to take was to investigate the conformational preferences of trinucleotides. In this paper, we report conformational and energetic data for a series of deprotonated T/G trinucleotides—$dGTT^-$, $dTGT^-$, and $dTTG^-$. These trinucleotides have the possibility of forming zwitterions like their tetranucleotide counterparts, but are easier to model and thus may be able to provide a clearer picture on the possible formation of zwitterions in the gas phase.

Experimental

Details concerning the experimental setup for the ion mobility measurements have been published [41] so only a brief description will be given here. Deprotonated trinucleotide ions were formed by MALDI in a home-built ion source [42]. Desalted samples of dGTT, dTGT, and dTTG were purchased from Sigma-Genosys (The Woodlands, TX) and used without further purification. 2,5-dihydroxybenzoic acid (DHB) was used as the matrix and methanol as the solvent. Approximately 100 μl of DHB (100 mg/ml) and 100 μl of the desired trinucleotide (~1 mg/ml) were applied to the sample target and dried. A nitrogen laser (λ = 337 nm, 1–2 mJ/pulse) was used to generate the ions in the MALDI source. The trinucleotide ion of interest, $[M - H]^-$, is mass selected in a double focusing, reverse geometry mass spectrometer and injected at low energies into a 4 cm long copper drift cell [41] filled with ~3 torr of helium. The temperature of the drift cell can be varied from 80 K to ~600 K. A weak, uniform electric field is applied across the cell that gently pulls the ions through the He gas at a constant drift velocity. Ions exiting the cell are detected as a function of time (the time is triggered by the laser pulse), yielding an arrival time distribution or ATD.

The mobility (K_o) of the ion is determined from a series of ATDs measured at different electric field strengths (5–25 V/cm) using eq 1

$$t_A = l^2 \frac{273}{760T}\left(\frac{1}{K_o}\frac{p}{V}\right) + t_o \quad (1)$$

where t_A is the measured arrival time, l is the length of the cell, T is temperature, p is the pressure of the He gas, V is the voltage across the cell, and t_o is the time the ion spends outside the drift cell [43]. A plot of t_A versus p/V yields a straight line with a slope inversely proportional to K_o. From the mobility, the ion–He collision cross-section, $\Omega^{(1,1)}$, can be obtained from eq 2

$$\Omega^{(1,1)} = \frac{C}{K_o} \quad (2)$$

where C contains known data about temperature, pressure, the ion–He reduced mass, and the ion charge [43]. Thus, the ion's arrival time is directly proportional to its collision cross-section and contains information about the geometric shape of the ion. Ions that are tightly folded have smaller cross-sections than ions that are more extended and, therefore, will have shorter arrival times. If the ion has multiple conformations that have significantly different cross-sections, each conformer may be separated from the others in the drift cell and appear as different peaks in the ATDs [38, 44–46] (assuming the conformers do not rapidly interconvert as they drift through the cell [39, 40, 47]).

Various computational methods are then used to generate candidate structures of the ions and calculate their collision cross-sections with He for comparison to experiment. For the trinucleotides presented here, molecular mechanics/dynamics calculations, using the AMBER 6.0 set of programs [48], were used to create the model structures. Typically, 150 low-energy structures of each trinucleotide ion are generated using a simulated annealing procedure. In this procedure, an initial structure is first energy minimized. This is followed by a 30 ps molecular dynamics simulation at 800 K and

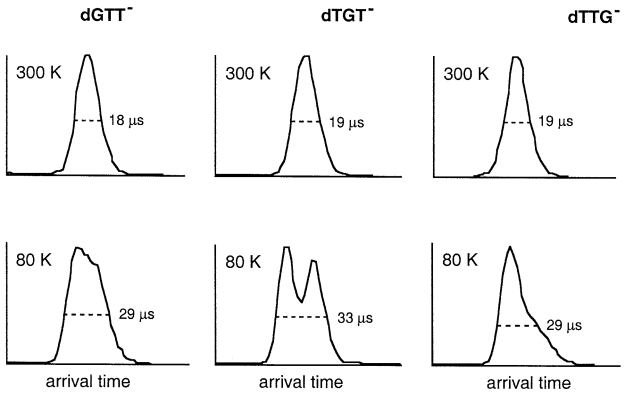

Figure 1. ATDs for $dGTT^-$, $dTGT^-$, and $dTTG^-$ obtained at a drift cell temperature of 300 K (top) and 80 K (bottom). The multiple peaks at 80 K represent different conformations of the ion. The expected peak width for a single conformer at 80 K is ~15 μs.

another 10 ps molecular dynamics simulation in which the temperature is gradually reduced to 0 K. The resulting structure is energy minimized again, saved, and used as the starting structure for another dynamics/minimization cycle. The entire process is repeated until 150 structures are obtained. Angle-averaged collision cross-sections of each structure are calculated using a temperature-dependent projection model [42, 49] that has proven reliable for biological [25–27] and synthetic [42, 47, 50–53] polymer systems with similar sizes as the trinucleotides. A scatter plot of cross-section versus relative energy for the 150 theoretical structures is then used to help identify the confomer(s) observed in the ATDs.

Results and Discussion

Arrival time distributions (ATDs) for $dGTT^-$, $dTGT^-$, and $dTTG^-$ measured at drift cell temperatures of 300 K and 80 K are shown in Figure 1. Single, symmetric peaks are present in all of the 300 K ATDs but multiple peaks appear in the 80 K ATDs. The relative intensity and degree of separation of the 80 K peaks are sequence dependent. For $dGTT^-$ and $dTGT^-$, the 80 K ATD peaks are approximately equal in intensity but for $dTTG^-$, the shorter-time peak is 2–3 times larger than the longer-time peak. In addition, two 80 K peaks are clearly observed for $dTGT^-$ but the ATDs for $dGTT^-$ and $dTTG^-$ only show shoulders on the long-time side of the main peak.

Multiple peaks in ATDs signify the presence of multiple conformers with significantly different collision cross-sections. For $dTGT^-$, the time difference between the two 80 K ATD peaks reflects a difference in cross-section of 17 ± 2 Å^2 (with the longer-time peak representing the conformer with the larger cross-section). Since two peaks are observed at 80 K but not at 300 K, the two conformers must be rapidly isomerizing at higher temperatures, yielding a single, time-averaged ATD peak. (This will be discussed in more detail later.)

Table 1. Experimental and Theoretical Cross-Sections (Å^2) for $dTGT^-$, $dTTG^-$, and $dTTG^-$

	Experiment		Theory (300K)	
	80K	300K	zwitterion	Non-zwitterion
dTGT	238, 255	196	180	189[a], 206[b]
dGTT	240,—[c]	194		190[a], 208[b]
dTTG	239,—[c]	195		188[a], 205[b]

[a]Folded conformer.
[b]Open conformer.
[c]A more extended conformer is observed but a precise cross-section could not be measured.

For each trinucleotide, a series of ATDs were measured at different drift voltages. From these measurements, accurate values of the mobilities of the ions are determined and converted to cross-sections using eqs 1 and 2. These cross-sections are listed in Table 1. All three trinucleotides have similar experimental cross-sections, regardless of sequence, suggesting that they may have similar conformations as well. (The increase in cross-section from 300 K to 80 K is due to the ion–He interaction potential, which has been described in detail elsewhere [49, 54]). Thus, if $dTGT^-$ is a zwitterion, it is not significantly more "open" or "folded" than $dGTT^-$ and $dTTG^-$, which are not expected to be zwitterions.

Normally, conformational identification of the ions is made by directly comparing the calculated cross-sections of theoretical structures to experimental values obtained from the ATDs. However, this sort of comparison is difficult for these systems. Multiple conformers are present for the trinucleotides and the ion mobility experiments can only separate them and give absolute cross-sections of each one at 80 K. At higher temperatures, the conformers isomerize as they travel through the drift cell resulting in a "time-averaged" conformation with an experimental cross-section that should fall somewhere between the values of the two "pure" forms. Unfortunately, we do not have accurate multidimensional surfaces for these trinucleotides and so the calculated cross-sections at 80 K are more uncertain than they are at 300 K where the ion-He interaction potential has little effect. Therefore, absolute cross-section comparisons between experiment and theory at 80 K are not useful but relative cross-section differences between two conformers can still be made and are the basis for our structural assignments.

dTGT

As mentioned previously, the main goal of this study is to determine whether these trinucleotides, $dTGT^-$ in particular, form zwitterions in the gas phase. Therefore, $dTGT^-$ was theoretically modeled assuming a zwitterionic and non-zwitterionic structure, shown in Figure 2. In the zwitterionic form, guanine (G) is protonated at N7 while the two phosphate groups are deprotonated. In the non-zwitterionic form, G is not protonated and only one of the phosphate groups is deprotonated. For

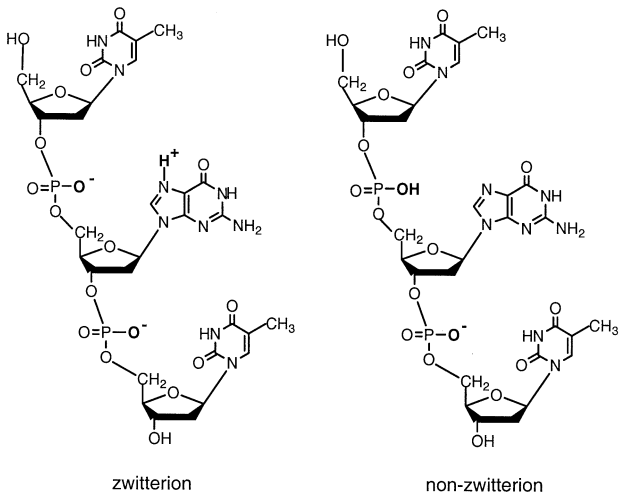

Figure 2. Diagram of the zwitterionic and non-zwitterionic forms of $dTGT^-$. In the non-zwitterion, either phosphate group can be deprotonated.

each case, a series of annealings and energy minimizations were used to create 150 candidate structures. The cross-section of each structure was then calculated and a scatter plot of cross-section versus energy used to help compare theory with experiment.

The scatter plot for the zwitterionic form of $dTGT^-$ is shown in Figure 3. Each point in the plot represents one theoretical structure and the cross-sections were calculated using a temperature of 300 K. The lowest energy structures are the most compact and have an average cross-section of 180 $Å^2$. This value is about 8% smaller than the experimental cross-section derived from the 300 K ATDs (see Table 1). Figure 4 shows the conformer that corresponds to these lowest energy points in the scatter plot. In this conformation, the two thymine (T) bases are stacked and the guanine (G) base is folded toward this stacked pair. The thymines stack so that the O4 carbonyl oxygen on one T is situated over the NH group on the other T. The T bases are not parallel but rather tilt toward each other so that NH · · · O=C hydrogen bonds form. This structural element was also observed for dinucleotides [39, 40]. Guanine also hydrogen bonds to one of the thymine bases (in this case, the 5'T) through the NH_2 group on G and the other carbonyl oxygen (O2) on T.

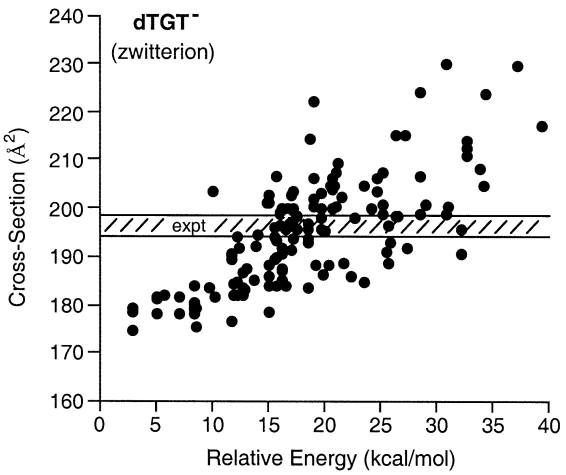

Figure 3. Scatter plot for the zwitterionic form of $dTGT^-$. Each point represents one theoretical structure generated from the molecular mechanics/dynamics calculations. The shaded horizontal bar represents the experimental cross-section determined from the 300 K ATDs (196 ± 2 $Å^2$).

A few problems arise with this zwitterionic structure. First, the extra H^+ on the N7 atom in guanine, which should be close to both phosphate groups in order to stabilize the proposed zwitterion, is more than 6 Å away from the 3' phosphate group (see the schematic diagram in Figure 4). Molecular dynamics simulations at 600 K (run for 1ns) indicate that the H^+ on guanine never gets closer than 6 Å to the 3' phosphate oxygens. The extra H^+ does, however, stay within 2 Å of the 5' phosphate oxygen during the entire dynamics run. Similar results were obtained from calculations on the zwitterionic structures of the tetranucleotides dTGTT$^-$ and dTTGT$^-$. The extra H^+ on guanine never bridged two deprotonated phosphate groups, but did remain close to the phosphate group on the 5' side of guanine.

The second problem is that theory predicts only one low-energy conformation for the $dTGT^-$ zwitterion, but the ion mobility experiments clearly indicate that two conformers exist whose cross-sections differ by ~17 $Å^2$. While the effect of the ion–He interaction potential on the cross-sections of the two conformers may be slightly different for each conformer, it is not drastically different either. Therefore, if the conformers never interconverted, their relative difference in cross-section should still be ~17 ± 3 $Å^2$ at 300 K (This was observed for dinucleotides in which two conformers could be separated as high as 200–300 K. The relative difference in cross-section between the two forms at 200 K was similar to the difference observed in the 80 K ATD data. Additionally, temperature dependent cross-section measurements of different sized synthetic polymers

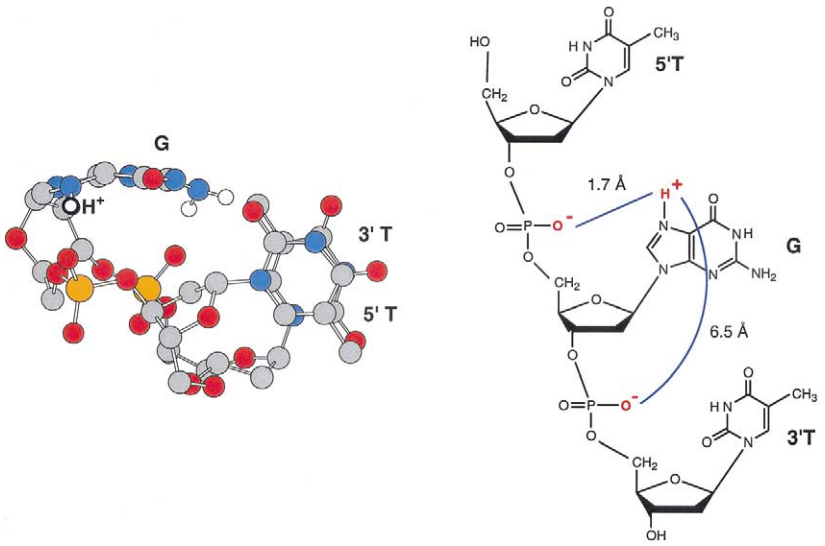

Figure 4. Lowest energy structure found for the zwitterionic form of $dTGT^-$. Carbons are gray, oxygens are red, nitrogens are blue, and phosphorous is orange. The extra H^+ on guanine is highlighted. The two thymine bases are stacked and the guanine base folds toward them so that the NH_2 group on G hydrogen bonds to the O2 carbonyl atom on T. The diagram shows the H···O distances between the extra H^+ on guanine and the two phosphate groups.

(i.e., 7-mer versus 12-mer) showed that relative differences measured at 300 K were similar to those measured at 100 K. See references [40, 42, 49, 51, 52]). However, the only structures in the scatter plot for the zwitterion that have ~17 $Å^2$ different cross-sections are also 10–15 kcal/mol different in energy. It is unlikely that a given conformer would rapidly convert into a 10–15 kcal/mol less stable conformation at room temperature. Even if they did, the cross-sections predicted for the zwitterions are too small to fit with any experimental data.

At 300 K, the ion mobility measurements yield an "average" cross-section due to the two conformers rapidly interconverting in the drift cell. This experimental cross-section should fall between the actual values of the two "pure" conformers. If $dTGT^-$ is a zwitterion, theory should predict two conformers that differ in cross-section by ~17 $Å^2$ and the 300 K experimental cross-section should be between the two theoretical values. The calculated cross-section for the lowest energy zwitterionic form of $dTGT^-$ is 180 ± 2 $Å^2$. The "second" zwitterionic conformer would need a cross-section of ~197 $Å^2$ in order to fit with the 17 $Å^2$ difference observed in the 80 K ATDs. Therefore, if two zwitterionic structures were present, the 300 K experimental cross-section for $dTGT^-$ should be between 180 $Å^2$ and 197 $Å^2$. The actual 300 K experimental cross-section for $dTGT^-$ is 196 ± 2 $Å^2$. The only way the theoretical zwitterionic structures could fit the 300 K experimental data was if the 10–15 kcal/mol higher energy conformers (with ~197 $Å^2$ cross-section) were the dominant forms and thus shifted the "averaged" 300 K cross-section towards their "pure" value (see reference [40]). This does not make sense energetically and does not fit in with the 80 K ATDs that show equal proportions of the two $dTGT^-$ conformers. Thus, $dTGT^-$ does not appear to be a zwitterion.

The other option for $dTGT^-$ is a non-zwitterionic structure in which G is not protonated and just one of the phosphate groups is deprotonated. The phosphate group on the 5' side of G or the 3' side of G can be deprotonated and both possibilities were considered in the modeling. Figure 5 shows the resulting scatter plots for the two non-zwitterionic forms of $dTGT^-$. Similar plots are observed for each deprotonated species but they are quite different than the one predicted for the zwitterion. Instead of one group of low-energy conformers as seen for the zwitterion, two families of low-energy conformers are predicted for the non-zwitterions (circled in Figure 5). These sets of conformers have similar energies but differ in cross-section by 18 ± 3 $Å^2$.

Representatives of each family are shown in Figure 6. The structures shown in this figure are deprotonated at the 5' phosphate but theory predicts similar conformers for the $dTGT^-$ ions with a deprotonated 3' phosphate. Unlike the zwitterion in which the two thymines stacked, G and T stack in the non-zwitterions. (In Figure 6, G stacks with the 5' T, but other structures in each family were observed in which G stacks with the 3' T.) The other T either folds towards this stacked pair (folded conformer, smaller cross-section) or extends away from it (open conformer, larger cross-section). In both families, the T/G stacked bases are angled towards each other with the NH group on one base hydrogen-bonded to a carbonyl oxygen on the other base. In the folded conformer, a hydrogen bond is also formed between the NH_2 group on G and the O4 carbonyl oxygen on the unstacked T. In the open conformer, the NH_2 group on G is hydrogen bonded to the deproto-

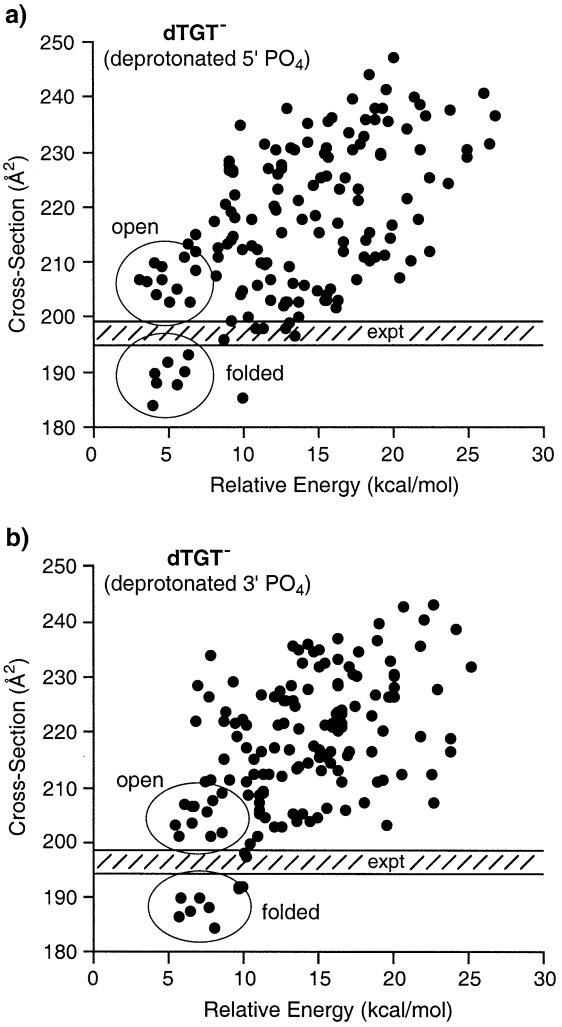

Figure 5. Scatter plots for the non-zwitterionic forms of $dTGT^-$ in which the 5' phosphate (**a**) and 3' phosphate (**b**) is deprotonated. The circled points represent two families of conformers shown in Figure 6. The shaded horizontal bar represents the experimental cross-section determined from the 300 K ATDs (196 ± 2 Å^2). Note that the experimental value falls between the values predicted for the two families of conformers.

nated phosphate group. Another structural feature common for both families of conformers is that the OH groups on each end of the oligonucleotide chain hydrogen-bond to the deprotonated phosphate group. The average cross-sections of the folded and open families are given in Table 1.

Unlike the zwitterion, the theoretical data for the non-zwitterions fit nicely with the ion mobility results. As can be seen in Table 1 as well as the scatter plots, the relative difference in cross-section predicted for the folded and open conformers (18 ± 3 Å^2) agrees very well with the experimental value determined from the two 80 K ATD peaks (17 ± 2 Å^2). Thus, the two peaks in the 80 K ATD can be reasonably assigned as the "non-zwitterionic" folded (faster time) and open (slower time) forms. At 300 K, where only one peak is observed in the ATD, the experimental cross-section for $dTGT^-$ (shown as the shaded horizontal bar in Figure 5) falls between the theoretical values of the folded and open form. This result also agrees nicely with the idea that the folded and open conformers are isomerizing at higher temperatures.

At 300 K, there is enough internal energy in the system to overcome the isomerization barrier between the folded and open forms. Therefore, the two conformers can rapidly interconvert as they drift through the cell resulting in a single, "time-averaged" conformation with a drift time (and hence cross-section) between that of the pure folded and open conformers. As the temperature in the drift cell is lowered, the internal energy in the system drops and the rate of the isomerization slows down. At sufficiently low temperatures, the internal energy in the system drops below the barrier height and the isomerization stops, effectively "freezing out" the two conformers. Figure 7 shows a series of ATDs for $dTGT^-$ measured at drift cell temperatures between 110 K and 170 K that demonstrates this isomerization process. The different shapes of the temperature-dependent ATDs can be fit using a model based on kinetic theory of ions in gases [55]. The only unknown variables in the fit are the rate constant for the folded → open transition (k_f) and the rate constant for the open → folded transition (k_o). Once k is known as a function of temperature, an Arrhenius plot of lnk versus $1/T$ should yield a straight line with a slope proportional to the barrier height. Figure 8 shows the data for $dTGT^-$ (following the folded → open rate constant), which yield a barrier height of 1.2 ± 0.2 kcal/mol.

dGTT and dTTG

Because the post source decay spectra for $dGTTT^-$ and $dTTTG^-$ showed the predicted loss of G, these tetranucleotides were not proposed to be stabilized by zwitterion formation [18]. Therefore, $dGTT^-$ and $dTTG^-$ are not expected to be zwitterions and were not modeled as such here. However, $dGTT^-$ and $dTTG^-$ can be deprotonated at the 5' or 3' phosphate and both options were considered. The scatter plots for these two trinucleotides are very similar to the ones generated for the non-zwitterionic forms of $dTGT^-$ shown in Figure 5. Two clusters of points within 1–2 kcal/mol of each other but with 18 ± 3 Å^2 different cross-sections are observed. The conformers corresponding to these two groups are also similar to the two conformers predicted for $dTGT^-$ shown in Figure 6. In the smaller cross-section group, G stacks with one of the T bases while the other T folds towards the stacked pair (folded conformer). In the larger cross-section group, G again stacks with one of the T bases but the other T extends away from this stacked pair (open conformer). As with $dTGT^-$, the site of the deprotonation (3' or 5' phosphate group) does not significantly alter the types of folded and open conformers predicted for $dGTT^-$ and $dTTG^-$. The average cross-sections of the folded and open conformers (calculated at 300 K) are given in Table 1.

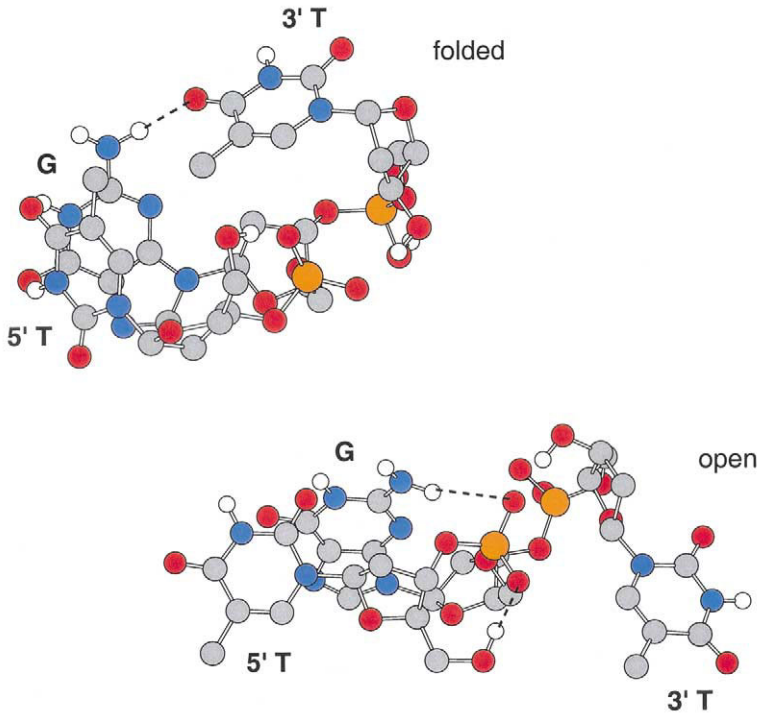

Figure 6. Representatives of the two families of dTGT$^-$ conformers observed in the scatter plots in Figure 5. In each case, guanine stacks with one of the thymine bases while the other thymine folds towards the stacked pair (folded) or away from it (open). In this figure the 5' phosphate group is deprotonated, but similar conformers are observed if the 3' phosphate is deprotonated. Various hydrogen bonds are shown with dotted lines.

The only significant differences between dGTT$^-$, dTGT$^-$, and dTTG$^-$ are the degree of separation of the multiple peaks in the 80 K ATDs and the relative intensity of the long-time peak in the dTTG$^-$ ATD. The ATD peaks are not as clearly separated for dGTT$^-$ and dTTG$^-$ as they are for dTGT$^-$, although none of the peaks are baseline resolved. However, the cross-section obtained for the shorter-time peak is the same for all three trinucleotides (accurate values of the long-time peak for dGTT$^-$ and dTTG$^-$ could not be obtained). The two peaks in the dTGT$^-$ ATD have been assigned to the folded (shorter-time) and open (longer-time) conformers. Based on the reasoning described in the previous section for dTGT$^-$ and the fact that the experimental cross-sections and theoretical structures are the same for all three trinucleotides, the peaks in the 80 K ATDs for dGTT$^-$ and dTTG$^-$ can also be reasonably assigned to the folded and open conformers. The only difference is that the isomerization barriers between the two conformers for dGTT$^-$ and dTTG$^-$ are not as high as the one for dTGT$^-$. Thus, the rate of isomerization between the folded and open forms at 80 K is faster for dGTT$^-$ and dTTG$^-$ than for dTGT$^-$. Unfortunately, accurate fits of temperature-dependent ATDs for dGTT$^-$ and dTTG$^-$ could not be obtained to determine the exact height of this barrier, but the values should not be too much smaller than the 1.2 kcal/mol determined for dTGT$^-$.

Summary

Ion mobility experiments and molecular mechanics/dynamics calculations were used to investigate the gas-phase conformations of deprotonated dGTT$^-$, dTGT$^-$, and dTTG$^-$ ions. The results indicate that dTGT$^-$ is not a stable zwitterion in the gas phase. The extra proton on G does not bridge the two deprotonated phosphates and the theoretical structures predicted for the zwitterionic form of dTGT$^-$ do not correlate with the ion mobility data. If however, dTGT$^-$ is modeled as a singly deprotonated species (irrespective of which phosphate group is deprotonated), theoretical and experimental results agree very well with each other. Two conformers are observed in the 80 K ATDs whose cross-sections differ by 17 ± 2 Å^2. Theory also predicts two conformers with 18 ± 3 Å^2 different cross-sections (at 300 K): a "folded" conformation in which G stacks with one of the T bases and the other T folds towards this stacked pair and an "open" conformation in which the other T extends away from the T/G stacked pair. At 300 K, these two conformers rapidly interconvert as they drift through the drift cell, yielding a single, time-averaged conformation with a cross-section between the values predicted for the folded and open conformers. Fitting the shapes of temperature-dependent ATDs yielded rate constants for the isomerization

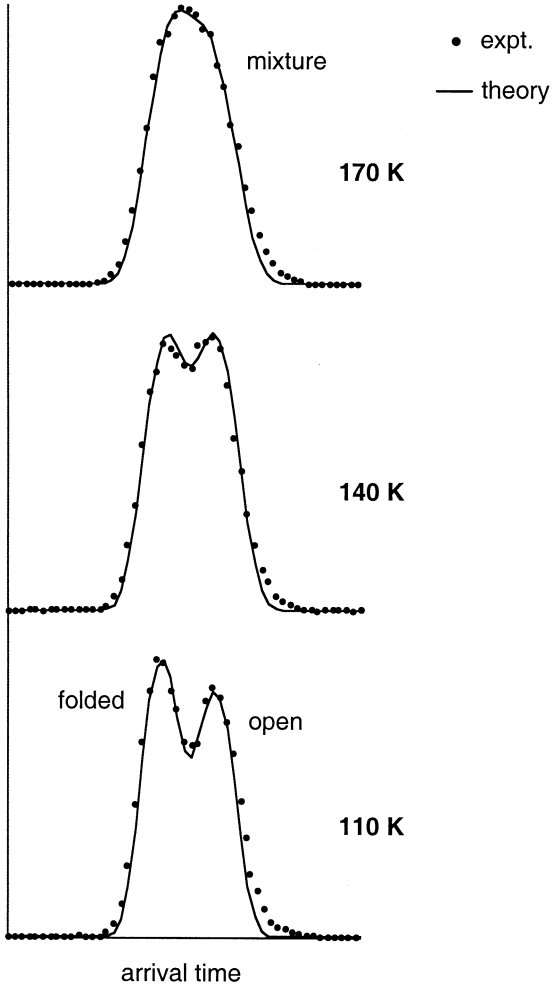

Figure 7. ATDs for $dTGT^-$ at different drift cell temperatures. The dots are experimental data while the lines are fits using the procedure outlined in the text. The only unknown variables in the fits are the folded → open and open → folded rate constants. The shape of the ATD depends on how fast the folded and open conformers interconvert as they drift through the cell.

process and an Arrhenius analysis of the data yielded a 1.2 kcal/mol isomerization barrier.

Similar folded and open conformers and cross-sections were also determined for $dGTT^-$ and $dTTG^-$ (which are not believed to be zwitterions), providing further evidence that $dTGT^-$ is not a zwitterion. The only significant differences between the three trinucleotides are the lower folded ↔ open isomerization barriers for $dGTT^-$ and $dTTG^-$ compared to $dTGT^-$ (as evidenced by lower degrees of separation between the 80 K ATD peaks) and the relatively larger abundance of the folded conformer observed in the $dTTG^-$ ATDs.

Acknowledgments

The authors gratefully acknowledge the support of the National Science Foundation under grants CHE9729146 and CHE0140215. They also thank Professor Franz Hillenkamp for initially suggesting we investigate zwitterion formation in oligonucleotides.

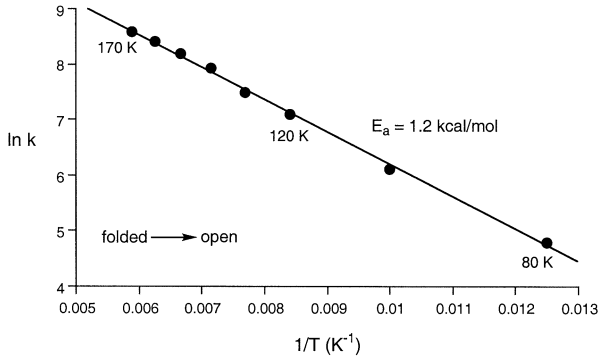

Figure 8. Arrhenius plot for $dTGT^-$ following the folded → open transition. *k* is determined from fits of the ATDs shown in Figure 7. The slope of the line is proportional to the isomerization barrer height (E_a). The estimated error is ~10%.

References

1. Koomen, J. M.; Russell, W. K.; Tichy, S. E.; Russell, D. H. Accurate Mass Measurement of DNA Oligonucleotide Ions Using High-Resolution Time-of-Flight Mass Spectrometry. *J. Mass Spectrom.* **2002,** *37,* 357–371.
2. Hofstadler, S. A.; Griffey, R. H. Analysis of Noncovalent Complexes of DNA and RNA by Mass Spectrometry. *Chem. Rev.* **2001,** *101,* 377–390.
3. Guo, B. C. Mass Spectrometry in DNA Analysis. *Anal. Chem.* **1999,** *71,* 333R–337R.
4. Karas, M.; Bachman, D.; Bahr, U.; Hillenkamp, F. Matrix-Assisted Ultraviolet Laser Desorption of Non-Volatile Compounds. *Int. J. Mass Spectrom. Ion Processes* **1987,** *78,* 53–68.
5. Wu, K. J.; Steding, A.; Becker, C. H. Matrix-Assisted Laser Desorption Time-of-Flight Mass Spectrometry of Oligonucleotides Using 3-Hydroxypicolinic Acid as an Ultraviolet-Sensitive Matrix. *Rapid Commun. Mass Spectrom.* **1993,** *7,* 142–146.
6. Nordhoff, E.; Cramer, R.; Karas, M.; Hillenkamp, F.; Kirpekar, F.; Kristiansen, K.; Roepstorff, P. Ion Stability of Nucleic Acids in Infrared Matrix-Assisted Laser Desorption Ionization Mass Spectrometry. *Nucleic Acids Res.* **1993,** *21,* 3347–3357.
7. Wu, K. J.; Shaler, T. A.; Becker, C. H. Time-of-Flight Mass Spectrometry of Underivatized Single-Stranded DNA Oligomers by Matrix-Assisted Laser Desorption. *Anal. Chem.* **1994,** *66,* 1637–1645.
8. Cheng, S.-W.; Chan, T.-W. D. Use of Ammonium Halides as Co-Matrices for Matrix-Assisted Laser Desorption/Ionization Studies of Oligonucleotides. *Rapid Commun. Mass Spectrom.* **1996,** *10,* 907–910.
9. Nordhoff, E.; Kirpekar, F.; Roepstorff, P. Mass Spectrometry of Nucleic Acids. *Mass Spectrom. Rev.* **1997,** *15,* 67–138.
10. Li, Y.; Cheng, S.; Chan, D. Evaluation of Ammonium Salts as Co-Matrices for Matrix-Assisted Laser Desorption/Ionization Mass Spectrometry of Oligonucleotides. *Rapid Commun. Mass Spectrom.* **1998,** *12,* 993–998.
11. Asara, J. M.; Allison, J. Enhanced Detection of Oligonucleotides in UV MALDI MS Using the Tetraamine Spermine as a Matrix Additive. *Anal. Chem.* **1999,** *71,* 2866–2870.
12. Berkenkamp, S.; Kirpekar, F.; Hillenkamp, F. Infrared MALDI Mass Spectrometry of Large Nucleic Acids. *Science* **1998,** *281,* 260–262.
13. Menzel, C.; Berkenkamp, S.; Hillenkamp, F. Infrared Matrix-Assisted Laser Desorption/Ionization Mass Spectrometry with a Transversely Excited Atmospheric Pressure Carbon Dioxide Laser at 10.6 μm Wavelength with Static and Delayed Extraction. *Rapid Commun. Mass Spectrom.* **1999,** *13,* 26–32.
14. Schneider, K.; Chait, B. T. Matrix-Assisted Laser Desorption Mass Spectrometry of Homopolymer Oligodeoxyribonucleoti-

des—Influence of Base Composition on the Mass Spectrometric Response. *Org. Mass Spectrom.* **1993,** *28,* 1353–1361.
15. Zhu, L.; Parr, G. R.; Fitzgerald, M. C.; Nelson, C. M.; Smith, L. M. Oligodeoxynucleotide Fragmentation in MALDI/TOF Mass Spectrometry Using 335-nm Radiation. *J. Am. Chem. Soc.* **1995,** *117,* 6048–6056.
16. Nordhoff, E.; Karas, M.; Cramer, R.; Hahner, S.; Hillenkamp, F.; Kirpekar, F.; Lezius, A.; Muth, J.; Meier, C.; Engels, J. W. Direct Mass Spectrometric Sequencing of Low-Picomole Amounts of Oligodeoxynucleotides with Up to 21 Bases by Matrix-Assisted Laser Desorption/Ionization Mass Spectrometry. *J. Mass Spectrom.* **1995,** *30,* 99–112.
17. Gross, J.; Leisner, A.; Hillenkamp, F.; Hahner, S.; Karas, M.; Schafer, J.; Lutzenkirchen, F.; Nordhoff, E. Investigations of the Metastable Decay of DNA Under Ultraviolet Matrix-Assisted Laser Desorption/Ionization Conditions with Post-Source-Decay Analysis and Hydrogen/Deuterium Exchange. *J. Am. Soc. Mass Spectrom.* **1998,** *9,* 866–878.
18. Gross, J.; Hillenkamp, F.; Wan, K. X.; Gross, M. L. Metastable Decay of Negatively Charged Oligodeoxynucleotides Analyzed with Ultraviolet Matrix-Assisted Laser Desorption/Ionization Post-Source-Decay and Deuterium Exchange. *J. Am. Soc. Mass Spectrom.* **2001,** *12,* 180–192.
19. Wan, K. X.; Gross, J.; Hillenkamp, F.; Gross, M. L. Fragmentation Mechanisms of Oligodeoxynucleotides Studied by H/D Exchange and Electrospray Ionization Tandem Mass Spectrometry. *J. Am. Soc. Mass Spectrom.* **2001,** *12,* 193–205.
20. Greco, F.; Ligouri, A.; Sindona, G.; Uccella, N. Gas-Phase Proton Affinity of Deoxyribonucleosides and Related Nucleobases by Fast Atom Bombardment Tandem Mass Spectrometry. *J. Am. Chem. Soc.* **1990,** *112,* 9092–9096.
21. Tsaprailis, G.; Nair, H.; Somogyi, A.; Wysocki, V. H. Influence of Secondary Structure on the Fragmentation of Protonated Peptides. *J. Am. Chem. Soc.* **1999,** *121,* 5142–5154.
22. Tsaprailis, G.; Somogyi, A.; Nikolaev, E. N.; Wysocki, V. H. Refining the Model for Selective Cleavage at Acidic Residues in Arginine-Containing Protonated Peptides. *Int. J. Mass Spectrom.* **2000,** *195/196,* 467–479.
23. Jonsson, A. P.; Bergman, T.; Jornvail, H.; Griffiths, W. J.; Bratt, P.; Stromberg, N. Gln-Gly Cleavage: Correlation Between Collision Induced Dissociation and Biological Degradation. *J. Am. Soc. Mass Spectrom.* **2001,** *12,* 337–342.
24. Griffiths, W. J.; Jonsson, A. P. Gas-Phase Conformation Can Have an Influence on Peptide Fragmentation. *Proteomics* **2001,** *1,* 934–945.
25. Wyttenbach, T.; von Helden, G.; Bowers, M. T. Gas-Phase Conformation of Biological Molecules—Bradykinin. *J. Am. Chem. Soc.* **1996,** *118,* 8355–8364.
26. Wyttenbach, T.; Batka, J. J.; Gidden, J.; Bowers, M. T. Host/Guest Conformations of Biological Systems: Valinomycin/Alkali Ions. *Int. J. Mass Spectrom.* **1999,** *193,* 143–152.
27. Wyttenbach, T.; Bushnell, J. E.; Bowers, M. T. Salt Bridge Structures in the Absence of Solvent? The Case for the Oligoglycines. *J. Am. Chem. Soc.* **1998,** *120,* 5098–5103.
28. Jarrold, M. F. Peptides and Proteins in the Vapor Phase. *Annu. Rev. Phys. Chem.* **2000,** *51,* 179–207.
29. Kinnear, B. S.; Hartings, M. R.; Jarrold, M. F. Helix Unfolding in Unsolvated Peptides. *J. Am. Chem. Soc.* **2001,** *123,* 5660–5667.
30. Kaleta, D. T.; Jarrold, M. F. Peptide Pinwheels. *J. Am. Chem. Soc.* **2002,** *124,* 1154–1155.
31. Counterman, A. E.; Clemmer, D. E. Cis-Trans Signatures of Proline-Containing Peptides in the Gas Phase. *Anal. Chem.* **2002,** *74,* 1946–1951.
32. Barnes, C. A. S.; Hilderbrand, A. E.; Valentine, S. J.; Clemmer, D. E. Resolving Isomeric Peptide Mixtures: A Combined HPLC/Ion Mobility—TOFMS Analysis of a 4000-Component Combinatorial Library. *Anal. Chem.* **2002,** *74,* 26–36.
33. Shelimov, K. B.; Clemmer, D. E.; Hudgins, R. R.; Jarrold, M. F. Protein Structure in Vacuo: Gas-Phase Conformations of BPTI and Cytochrome C. *J. Am. Chem. Soc.* **1997,** *119,* 2240–2248.
34. Badman, E. R.; Hoaglund-Hyzer, C. S.; Clemmer, D. E. Monitoring Structural Changes of Proteins in an Ion Trap Over ~10–200ms: Unfolding Transitions in Cytochrome C Ions. *Anal. Chem.* **2001,** *73,* 6000–6007.
35. Valentine, S. J.; Clemmer, D. E. Temperature-Dependent H/D Exchange of Compact and Elongated Cytochrome C Ions in the Gas Phase. *J. Am. Soc. Mass Spectrom.* **2002,** *13,* 506–517.
36. Hoaglund, C. S.; Liu, Y.; Ellington, A. D.; Pagel, M.; Clemmer, D. E. Gas-Phase DNA: Oligothymidine Ion Conformers. *J. Am. Chem. Soc.* **1997,** *119,* 9051–9052.
37. Bowers, M. T.; Kemper, P. R.; von Helden, G.; van Koppen, P. A. M. Gas-Phase Ion Chromatography—Transition Metal State Selection and Carbon Cluster Formation. *Science* **1993,** *260,* 1446–1451.
38. Clemmer, D. E.; Jarrold, M. F. Ion Mobility Measurements and Their Applications to Clusters and Biomolecules. *J. Mass Spectrom.* **1997,** *32,* 577–592.
39. Gidden, J.; Bushnell, J. E.; Bowers, M. T. Gas-Phase Conformations and Folding Energetics of Oligonucleotides: dTG^- and dGT^-. *J. Am. Chem. Soc.* **2001,** *123,* 5610–5611.
40. Gidden, J.; Bowers, M. T. Gas-Phase Conformational and Energetic Properties of Deprotonated Dinucleotides. *Eur. Phys. J. D.* **2002,** *20,* 409–419.
41. Kemper, P. R.; Bowers, M. T. A Hybrid Double-Focusing Mass Spectrometer—High-Pressure Drift Reaction Cell to Study Thermal Energy Reactions of Mass Selected Ions. *J. Am. Soc. Mass Spectrom.* **1990,** *1,* 197–207.
42. von Helden, G.; Wyttenbach, T.; Bowers, M. T. Inclusion of a MALDI Ion Source in the Ion Chromatography Technique—Conformational Information on Polymer and Biomolecular Ions. *Int. J. Mass Spectrom. Ion Processes* **1995,** *146/147,* 349–364.
43. Mason, E. A.; McDaniel, E. W. *Transport Properties of Ions in Gases.* Wiley: New York, 1988.
44. von Helden, G.; Hsu, M.-T.; Gotts, N.; Bowers, M. T. Carbon Cluster Cations with up to 84 Atoms—Structures, Formation Mechanism, and Reactivity. *J. Phys. Chem.* **1993,** *97,* 8182–8192.
45. Gotts, N. G. von; Helden, G.; Bowers, M. T. Carbon Cluster Anions—Structure and Growth from C_5^- to C_{62}^-. *Int. J. Mass Spectrom. Ion Processes* **1995,** *149/150,* 217–229.
46. Shvartsburg, A. A.; Hudgins, R. R.; Dugourd, P.; Jarrold, M. F. Structural Information from Ion Mobility Measurements: Applications to Semiconductor Clusters. *Chem. Soc. Rev.* **2001,** *30,* 26–35.
47. Gidden, J.; Wyttenbach, T.; Batka, J. J.; Weis, P.; Jackson, A. T.; Scrivens, J. H.; Bowers, M. T. Folding Energetics of Macromolecules in the Gas Phase: Alkali Ion-Cationized Poly(ethylene terephthalate) Oligomers. *J. Am. Chem. Soc.* **1999,** *121,* 1421–1422.
48. Case, D. A.; Pearlman, D. A.; Caldwell, J. W.; Cheatham, T. E., III; Ross, W. S.; Simmerling, C. L.; Dearden, T. A.; Merz, K. M.; Stanton, R. V.; Cheng, A. L.; Vincent, J. J.; Crowley, M.; Tsui, V.; Radner, R. J.; Duan, Y.; Pitera, J.; Massova, I.; Seibel, G. L.; Singh, U. C.; Weiner, P. K.; Kollman, P. A. *AMBER 6.* University of California: San Francisco, 1999.
49. Wyttenbach, T. von; Helden, G.; Batka, J. J., Jr.; Carlat, D.; Bowers, M. T. Effect of the Long Range Potential on Ion Mobility Measurements. *J. Am. Soc. Mass Spectrom.* **1997,** *8,* 275.
50. Wyttenbach, T.; von Helden, G.; Bowers, M. T. Conformations of Alkali Ion Cationized Polyethers in the Gas Phase: Polyethylene Glycol and Bis[(benzo-15-crown-5)-15-ylmethyl] Pimelate. *Int. J. Mass Spectrom.* **1997,** *165/166,* 377–390.

51. Gidden, J.; Jackson, A. T.; Scrivens, J. H.; Bowers, M. T. Gas-Phase Conformations of Synthetic Polymers: Poly(methyl methacrylate) Oligomers Cationized by Sodium Ions. *Int. J. Mass Spectrom.* **1999,** *188,* 121–130.
52. Gidden, J.; Wyttenbach, T.; Jackson, A. T.; Scrivens, J. H.; Bowers, M. T. Gas-Phase Conformations of Synthetic Polymers: Poly(ethylene glycol), Poly(propylene glycol), and Poly(tetramethylene glycol). *J. Am. Chem. Soc.* **2000,** *122,* 4692–4699.
53. Gidden, J.; Jackson, A. T.; Scrivens, J. H.; Bowers, M. T. Gas-Phase Conformations of Cationized Poly(styrene) Oligomers. *J. Am. Soc. Mass Spectrom.* **2002,** *13,* 499–505.
54. Shvartsburg, A. A.; Schatz, G. C.; Jarrold, M. F. Mobilities of Carbon Cluster Ions: Critical Importance of the Molecular Attractive Potential. *J. Chem. Phys.* **1998,** *108,* 2416–2423.
55. Gatland, I. R. Analysis for Ion Drift Tube Experiments. *Case Studies Atomic Phys.* **1974,** *4,* 369–437.